The effect of injectable platelet-rich fibrin in combination with autogenous bone grafts on bone healing in an ovariectomized osteoporotic rat model with critical-sized defects

Mustafa C. Durmuşlar, DDS, PhD, *Elif A. Gülşen,* DDS, PhD, *Kemal A. Bayburt,* DDS, PhD, *Umut Ballı,* DDS, PhD, *Mert Ocak,* PhD, *Ayşegül Fırat,* MD, PhD, *Elham B. Zırh,* PhD, *Hakan H. Çelik,* MD, PhD.

ABSTRACT

الأهداف: قيمت هذه الدراسة تأثير مواد الطعم الذاتي، بما في ذلك الطعم العظمي الذاتي المنشأ (ABG) وجلطات الفيبرين الغني بالصفائح الدموية القابلة للحقن (I-PRF)، على تجديد عيوب العظام في الفئران المصابة بهشاشة العظام المستأصلة من المبيض.

المنهجية: تم استئصال المبيض من فئران الويستار (بعمر 6-8 أسابيع)، وبدأت الجراحة بعد 8 أسابيع. تم إحداث عيب بطول 5 ملم في العظام الجدارية ل 16 جرذًا في كلا الجانبين، وتم تقسيمها إلى 4 مجموعات. كانت العيوب في المجموعة A (فارغة) غير معالجة؛ أما المجموعات ب، ج، د فقد تم ملء العيوب B 0.1 مل من I-PRF، و0.1 مل من ABG، ومزيج من 0.1 مل من كل من I-PRF وABG على التوالي. بعد 4 أسابيع من الجراحة، تم قتل الفئران قتلاً رحيمًا. تم تقييم تجدد العظام من خلال تحليل الأنسجة المرضية والتصوير المقطعي المحوسب الدقيق.

النتائج: في الفئران المستأصلة من المبيض التي عولجت بال ABG أو I-PRF، تم تعزيز تجدد العظام، مع زيادة نشاط السمحاق وعدد الخلايا البانية للعظم وحجم العظام الجديدة، كما تم تحديده من الناحية النسيجية. كان لدى مجموعة ABG+I-PRF أعلى أوعية سمحاقية، لكن الفرق بالمقارنة مع مجموعة ABG لم يكن ذا دلالة إحصائية (0.05<*p*). كانت أعداد الأرومات العظمية أعلى بشكل ملحوظ في مجموعة ABG+I-PRF مقارنة بالمجموعة الفارغة (0.05>*p*). أظهر التصوير المقطعي المحوسب الدقيق أعلى متوسط لنسبة حجم العظام الجديدة في مجموعة ABG+I-PRF، تليها مجموعة ABG.

الخلاصة: يعزز الاستخدام المشترك ل ABG و I-PRF من تكوين العظام في الفئران المصابة بهشاشة العظام بعد استئصال المبيض.

Objectives: To assess the impact of autogenous graft materials, including autogenous bone graft (ABG) and injectable platelet-rich fibrin (I-PRF) clots, on bone defect regeneration in ovariectomized osteoporotic rats.

Methods: Wistar rats (6-8 weeks old) were ovariectomized, and surgery began after 8 weeks. A 5-mm defect was created bilaterally in the parietal bones of 16 rats, which were divided into 4 groups. Group A (blank) had untreated defects; group B had defects filled with 0.1 ml of I-PRF, group C had defects filled with 0.1 ml of ABG, and group D had defects filled with a combination of 0.1 ml each of I-PRF and ABG. Four weeks post-surgery, the rats were euthanized. Bone regeneration was evaluated through histopathologic analysis and microcomputed tomography (micro-CT).

Results: In ovariectomized rats treated with ABG or I-PRF, bone regeneration was enhanced, with increased periosteal activity, osteoblast count, and new bone volume, as determined histologically. The ABG+I-PRF group had the highest periosteal vascularity, but the difference compared to the ABG group was not statistically significant (*p*>0.05). Osteoblast numbers were significantly higher in the ABG+I-PRF group than in the blank group (*p*<0.05). Micro-CT showed the highest mean new bone volume ratio in the ABG+I-PRF group, followed by the ABG group.

Conclusion: The combined use of ABG and I-PRF enhances bone formation in osteoporotic rats following ovariectomy.

Keywords: animal experiment, bone regeneration, osteoporosis, platelet rich fibrin

Address correspondence and reprint request to: Dr. Mustafa C. Durmuşlar, Department of Oral and Maxillofacial Surgery, Faculty of Dentistry Biruni University, Istanbul, Turkey. E-mail: mdurmuslar@biruni.edu.tr ORCID ID: https://orcid.org/0000-0002-0590-9788

Bone defects in the oral and maxillofacial region can occur for many reasons, such as tumor, infection, or trauma requiring surgery. Several types of bone substitutes are employed to repair bone defects, yet the healing process is also influenced by the characteristics of the host bone.[1]

Osteoporosis is the most common bone ailment in older adults. It is a chronic systemic condition characterized by decreased osteoblastic activity and increased osteoclast activity, leading to reductions in bone mass and bone mineral density in addition to a deterioration of the intricate micro-architecture within bone tissue.[2] This deterioration is primarily driven by an expansion of marrow spaces, thereby increasing bone fragility and, in turn, a susceptibility to fractures.[1]

Among the graft materials used to restore bone defects are autografts, allografts, xenografts, and alloplastic grafts, often supported by an autologous blood concentrate. Autogenous bone grafts (ABG) are widely regarded as the gold standard due to their exceptional osteogenic and osteoinductive qualities.[3] However, in bone metabolism disorders such as osteoporosis, bone healing is delayed and the quality of newly formed bone is often poor.[1]

Ehrenfest et al[4] categorized various platelet-rich plasma (PRP) and platelet-rich fibrin (PRF) formulations into 4 distinct groups according to their leukocyte and fibrin content: pure platelet-rich plasma (P-PRP), leukocyte- and platelet-rich plasma (L-PRP), pure platelet-rich fibrin (P-PRF), and leukocyte- and platelet-rich fibrin (L-PRF).[4,5] Ghanaati et al[6] introduced a novel PRF preparation, advanced platelet-rich fibrin (A-PRF), prepared using low-speed centrifugation. Advanced-PRF has a more relaxed fibrin scaffold, enhances cell penetration and attracts inflammatory cells and platelets.[6] Low-speed centrifugation has also been utilized in creating injectable PRF (I-PRF), a liquid platelet concentrate prepared in plastic tubes without adding anticoagulants, similar to PRF. Injectable-PRF provides several benefits, including the prolonged release of various growth factors such as trefoil factor family-β, platelet-derived growth factor (PDGF), and vascular endothelial growth factor, stimulation of local angiogenesis, improved stem cell adhesion, modulation of the immune response, and promotion of epithelial cell growth.[7] Injectable-PRF was also shown to have a more pronounced impact than PRP on the migration,

proliferation, differentiation of human osteoblasts, and on osteoblast behavior.[8] Injectable-PRF also contains a significantly higher number of platelets, leukocytes, monocytes, and granulocytes than other liquid blood concentrates such as plasma rich in growth factor and PRP.[9]

Both PRF and I-PRF have been used in dentistry as graft materials. Among the successful applications of I-PRF is as a membrane in implant surgery, the surgical treatment of malignant lesions, defect repair in periodontal surgery, the treatment of gum recession, post-tooth extraction healing, post-operative healing following jaw cyst surgery, and in sinus lift procedures.[10-14]

In this study, we utilized an ovariectomized rat model to assess the impact of I-PRF on bone regeneration and resorption following the application of an autogenous graft.

Methods. This study involved 16 Wistar rats aged 6-8 weeks. The animals were kept in standard cages under controlled conditions, with 40-60% humidity, a temperature of 22±1°C, and a 12-hour light/dark cycle. The animals were provided with standard laboratory food and water, available ad libitum. This study received approval from the institutional review board and ethical committee of Bülent Ecevit University, Zonguldak, Turkey, for experimental research on animals (approval date and number: 2023.13.13/07).

All surgical procedures were carried out under sterile conditions in an animal laboratory surgical suite. The rats were anesthetized using an intramuscular injection of 3 mg/kg xylazine hydrochloride (Rompuns, Bayer, Leverkusen, Germany) and 35 mg/kg ketamine hydrochloride (10% Ketasol; Richter Pharma AG, Wels, Austria). Bilateral ovariectomy was carried out on all animals. Lei et al[15] reported that an osteoporosis profile could be established 8 weeks post-procedure in ovariectomized animals. Based on their findings, we carried out bilateral ovariectomy on all animals. Our study commenced at the 8-week mark following the ovariectomy. Before creating the calvarial defects, 3 milliliters of blood were collected from each animal through cardiac puncture using a 5 mL disposable syringe (Berika®, Konya, Türkiye).[16] Injectable-PRF was prepared following a protocol of 700 RPM for 3 minutes (RCF-max ~60 g, RCF-clot ~52 g) using the Process for PRF Duo centrifugation device (40° rotor angulation, 95 mm radius at the clot, 110 mm at the maximum, Duo Centrifuge, Process For PRF, Nice, France) with 10 mL plastic tubes free of anticoagulant. The rats were prepared aseptically, followed by making a semilunar incision and reflecting a full-thickness flap to

expose the parietal and frontal bones. Bilateral critical size calvarial defects with a 5-mm diameter were created using a trephine and a low-speed handpiece, while ensuring continuous sterile saline irrigation. Special care was taken during the surgery to avoid damaging the duramater. Bone from the region of the defect was carefully removed with the assistance of a periosteal elevator and then fragmented into small pieces in a sterile box. The resulting 0.1 ml of ABG and 0.1 ml of I-PRF were combined, or not, and applied as appropriate for groups A-D. After the defect had been filled with the material, the flap was closed using resorbable 4/0 polyglactin 910 sutures (Vicryl; Ethicon, Somerville, NJ, USA). For postoperative infection control, the rats were injected with 10 mg cefazolin (Sefazol; M Nevzat, Istanbul, Turkey); a metamizol sodium (Novalgin, Aventis, Turkey) was provided as analgesic for 5 days after surgery.

At 4 weeks post-surgery, the animals were euthanized using a lethal injection of anesthetics. The skin was dissected, and the calvaria were removed and promptly immersed in a 10% formaldehyde solution.

The power analysis for sample size calculation was carried out prior to the study initiation. Based on the results of the power analysis, it was determined that 8 rats were required for each group to achieve a 90% power level for type II error and a 5% probability level for type I error in detecting differences in new bone formation.[17]

Defects were created in both parietal areas of the skull. In 8 rats, one of the created defect areas was left blank, while in the contralateral defect I-PRF was applied. In the remaining 8 animals, one defect was treated with ABG alone, and the other with ABG+I-PRF. The 32 defect sites were therefore either left untreated or treated according to one of the 3 treatment protocols, resulting in 4 groups as follows: group A (blank group): flap closed without any intervention; group B (I-PRF group): defect filled with I-PRF; group C (ABG group): defect filled with an autogenous graft (prepared using a bone grinder); and group D (ABG/I-PRF): defect filled with 0.1 ml of ABG + 0.1 ml of I-PRF.

The samples intended for microcomputed tomography (micro-CT) analysis were scanned using a micro-CT (Skyscan 1174; Micro Photonics Inc., Allentown, PA, USA) device with the following settings: a spatial resolution of 15 μm, scanning parameters set at 50 kV and 800 μA, and a rotation step of 0.7° covering a total rotation of 180°. NRECON software was used to generate 3D images, and CTAn software was employed for data analysis. New mineralized bone volume was calculated by including only the bone, and none of the graft materials. The entire calvarial defect was considered as the region of interest. In each section, total tissue, new bone and graft were identified based on gray scale values (0-255 range) in addition to visual differences between the 3. While new bone was identified at a CT gray scale range of 15-70, total tissue 15-150 and bone greft 210-255 were identified in the range of 0-250 gray scale.

Bone tissues were prefixed with 10% buffered formalin, for 2 days, and decalcified using a rapid decalcification kit (RDC-1, Wellpath, Türkiye) according to the manufacturer's instructions. Decalcification was controlled by gentle tissue bending and was carried out for 7±2 days. The tissues were then post-fixed with buffered formalin for 10 days and processed using an automatic tissue processor (Leica TP-1020, IL, USA), and paraffin-embedded. Sections of 4- to 5-μm thickness were prepared from the blocks using a sliding microtome (Leica SM-2010, IL, USA) and then deparaffinized in a 60° oven overnight. The deparaffinized sections were rehydrated using graded ethanol solutions, stained with hematoxylin and eosin or Masson's trichrome stain, and mounted. For histopathologic evaluations, micrographs were taken at 4×, 10×, and 20× magnification (5 different randomly selected areas per sample). Images were analyzed for evidence of new bone formation, periosteal vascularity, and the number of osteoblasts, using an image analysis program (ImageJ, 1.53j, NIH, USA). The new bone area was calculated as μm2, and each group's mean values were determined. Periosteal vascularity (modification of the method described in Santić V et al[18]) and the number of osteoblasts in the new bone area of each section were determined. Then the mean values were determined for each group (**Figure 1**).

Statistical analysis. A Shapiro-Wilk test was carried out to determine the normality of the data. Periosteal vascularity, osteoblast count, and new bone formation were non-normally distributed and thus analyzed using a Kruskal-Wallis nonparametric test, followed by post-hoc group comparisons with the Bonferroni-adjusted Mann-Whitney U test. For the Bonferroni correction, $\alpha=0.05/6$; $p=0.008$ was considered to be statistically significant. All tests were carried out using the Statistcal Package for the Social Sciences software, version 19.0 (SPSS Inc., Chicago, IL, USA).

Results. The surgical procedures were well-tolerated by all animals, except for a single individual in the ABG and ABG+I-PRF groups, who encountered a setback during the post-surgical phase. Encouragingly, no signs of wound dehiscence, infection, or abscess formation were noted across any surgical sites, indicating a
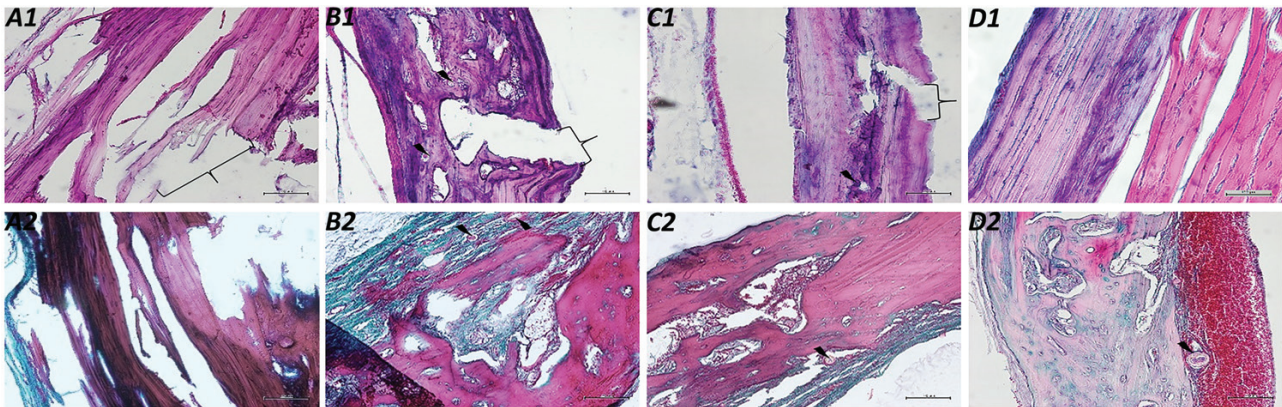
Figure 1 - Micrographs of sections from all groups with hematoxylin-eosin (**upper row**) and trichrome (**lower row**) staining. The Thunderbolt mark indicates grafts or graft-placed sites, and arrowheads indicate areas of non-healing bone fractures (the magnification is 200x). **A)** Indicates blank group; **B)** only injectable platelet-rich fibrin (I-PRF) group; **C)** only autologous bone graft (ABG) group; **D)** ABG/I-PRF groups.

successful recovery period for the majority of the experimental cohort.

The histological findings are depicted in **Figure 1**. Notably, there were no indications of inflammatory reactions or secondary infections at any of the surgical sites. The predominant component observed in both the blank and PRF groups was fibrous (collagenous) connective tissue. In all groups, new bone trabeculae were observed from the periphery toward the center of the defect (but not in the center). New bone also formed around the graft particles in all graft groups. The extent of new bone formation differed between the bone-grafted and non-bone-grafted groups (**Figure 1**).

Periosteal vascularity was highest in the ABG+I-PRF group (2.54±0.15), although it did not significantly differ from that in the ABG group (2.29±0.28, $p>0.05$), and was lowest in the blank group (0.58±0.13). The observed difference compared to the I-PRF group (1.45±0.21) was statistically significant ($p<0.05$). Similarly, a significant difference was noted between the ABG-treated and non-ABG-treated groups ($p<0.05$; **Figure 2**).

The average osteoblast count was the lowest in the blank group (0.70±0.19) and the highest in the ABG+I-PRF group (2.49±0.11, $p<0.05$). The difference between the blank group and the I-PRF group (1.53±0.15) in terms of the number of osteoblasts was significant ($p<0.05$), whereas the difference was between the I-PRF and ABG group (1.74±0.22) was not ($p>0.05$). The ABG/I-PRF and ABG groups also differed significantly ($p<0.05$; **Figure 3**).

Mean new bone volume was highest in the ABG+I-PRF group (182.03±7.50), followed by the ABG group (113.23±17.38); the difference was significant ($p<0.05$). The blank group had the lowest amount of
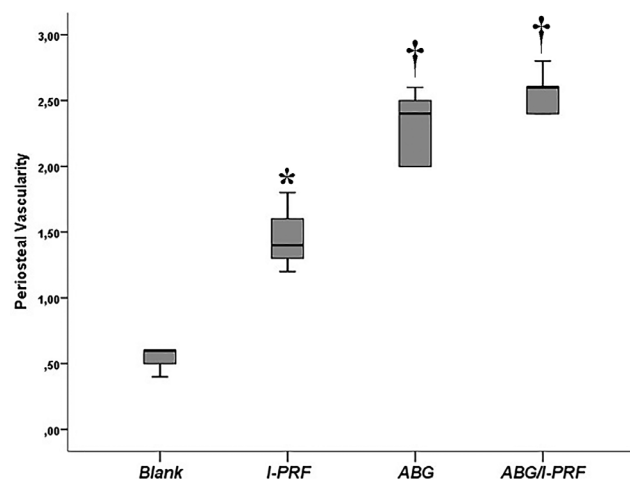

Figure 2 - Periostal vascularity in study groups. Periostal vascularity scoring was carried out as: 0=none, 1=mild, 2=moderate, and 3=severe. *Statistically significant difference from blank group. †Statistically significant difference from blank and injectable platelet-rich fibrin groups (Kruskal-Wallis/Bonferroni-adjusted Mann-Whitney U). Data are presented as box and whisker plots. The median value is indicated by the line within the box plot. The box extends from the 25-75th percentiles. Whiskers extend to show the highest and lowest values. I-PRF: injectable platelet-rich fibrin, ABG: autologous bone graft

new bone (71.25±7.18), and the difference compared with the I-PRF group (92.45±5.51) was significant ($p<0.05$). The difference between the ABG-treated and non-ABG-treated groups was also significant ($p<0.05$; **Figure 4**).

The average new bone volume ratio was highest in the ABG+I-PRF group (68.21±5.18), followed by the ABG group (59.08±4.11). The difference between these 2 groups was statistically significant ($p<0.05$). The blank group exhibited the lowest new bone volume ratio
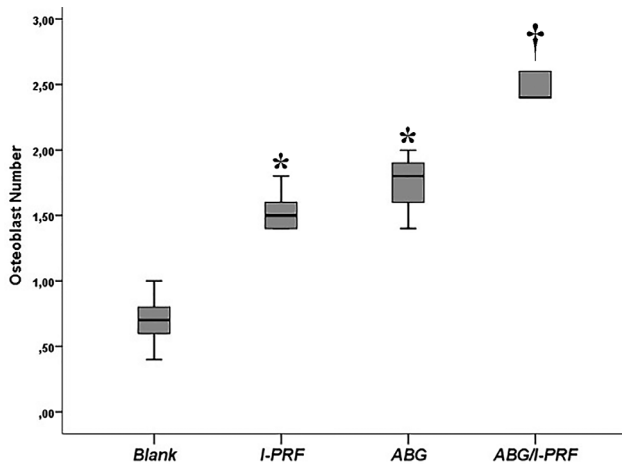
Figure 3 - Osteoblast number in study groups. Osteoblast count scoring was carried out as: 0=none, 1=mild, 2=moderate, and 3=severe. *Statistically significant difference from blank group. †Statistically significant difference from blank, injectable platelet-rich fibrin and autologous bone graft groups (Kruskal-Wallis/Bonferroni-adjusted Mann-Whitney U). Data are presented as box and whisker plots. The median value is indicated by the line within the box plot. The box extends from the 25-75th percentiles. Whiskers extend to show the highest and lowest values. I-PRF: injectable platelet-rich fibrin, ABG: autologous bone graft

Figure 4 - New bone volume in study groups. New bone formation area calculated as μm2. *Represents statistically significant difference (Kruskal-Wallis/Bonferroni-adjusted Mann-Whitney U). Data are presented as box and whisker plots. The median value is indicated by the line within the box plot. The box extends from the 25-75th percentiles. Whiskers extend to show the highest and lowest values. I-PRF: injectable platelet-rich fibrin, ABG: autologous bone graft

(35.47±6.3), with a statistically significant difference compared to the I-PRF group (48.48±5.76; *p*<0.05). The difference between the ABG and non-ABG groups was also found to be statistically significant (*p*<0.05; Figure 5).

Discussion. Osteoporosis, characterized by insufficient bone formation and excessive bone resorption, is a chronic condition that predominantly impacts older adults, and particularly women.[2] The decline in bone volume and density extends to the maxilla and mandible, with a concurrent increase in bone deterioration around the teeth.[1] Alleviating the metabolic disturbances associated with osteoporosis is challenging in terms of bone regeneration, with adverse effects on the patient's quality of life.[2] An improvement in bone grafting techniques in applications related to oral and maxillofacial surgery, with the goal of reducing bone healing time and the risk of complications as well as fostering the development of more mature bone, has been the focus of considerable research. Nonetheless, the regeneration of osteoporotic bone, including that facilitated by the implantation of biomaterials, has not been adequately evaluated.

This study investigated the effects of I-PRF on bone regeneration and resorption after applying an autogenous graft in an ovariectomized rat model.
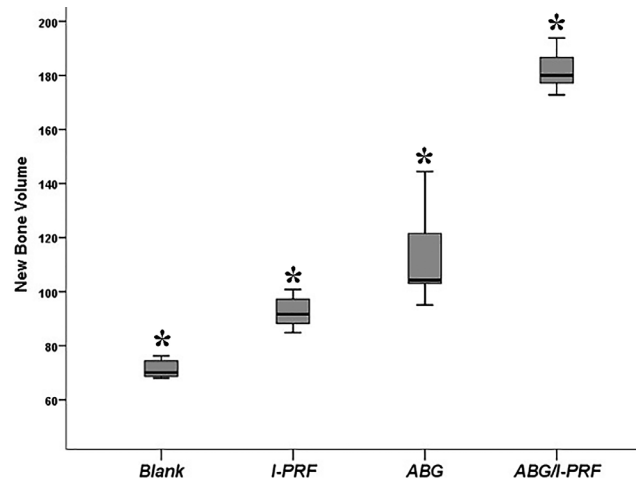

Figure 5 - New bone volume ratios in study groups. *Represents statistically significant difference (Kruskal-Wallis/Bonferroni-adjusted Mann-Whitney U). Data are presented as box and whisker plots. The median value is indicated by the line within the box plot. The box extends from the 25-75th percentiles. Whiskers extend to show the highest and lowest values. I-PRF: injectable platelet-rich fibrin, ABG: autologous bone graft
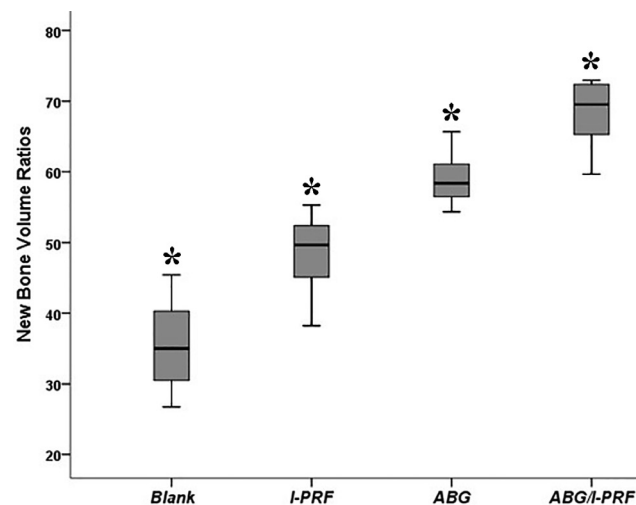
Micro-CT and histological analyses were employed to examine the new bone area, osteoblast numbers, and the quantity of newly formed bone in the defect sites during the early healing phase. Our results demonstrated the favorable outcomes achieved with the use of I-PRF in the grafting procedure.

The success of the biomaterials used in defect repair in osteoporosis models has been a topic of discussion. Oberg et al[19] created a 5mm diameter defects in the tibias of both ovariectomized and healthy rabbits. Half of the defects were treated with allogeneic bone grafts. After an 8-week period, histological assessments revealed no significant differences between the empty cavities and those treated with grafts. However, there was a notable disparity in new bone formation, with significantly less formed in the ovariectomized rabbits than in their healthy counterparts.[19] Ribeiro et al[20] treated surgically created defects in the femurs of ovariectomized rats with hydroxyapatite grafts. In the group not receiving hormone replacement therapy, histological analyses revealed the reduced presence of newly formed bone. Similar findings were reported using a comparable ovariectomized rat model. Durão et al[21] demonstrated a decrease in biomaterial-induced bone formation in ovariectomized rats, as evidenced by microtomographic and histological analyses. Additionally, compromised osteoblastic function in the regenerated bone was identified through gene expression analyses. The authors related their findings to the impaired osteogenic processes that occur in osteoporosis patients in the context of biomaterial-mediated bone healing.[21]

As a user-friendly platelet concentrate in liquid form, I-PRF can be employed independently or easily combined with a variety of biomaterials 6, 22. The high concentration of regenerative cells and growth factors present in I-PRF may lead to more successful bone and soft tissue regeneration, improved hemostasis, bone maturation and angiogenesis, and faster healing. Moreover, I-PRF is compatible with the body, can be prepared by centrifugation at slower and shorter speeds, and has recently been shown to have both antimicrobial and anti-inflammatory properties.[7,23,24]

In 2 studies carried out by Mu et al,[25] the effects of I-PRF modified with gelatin nanoparticles (GNPs) and deproteinized bovine bone mineral (DBBM) on sinus augmentation in rabbits were evaluated. Bone production in the region of the elevated Schneiderian membrane was shown to be notably higher in the sinus cavities treated with GNPs-I-PRF hydrogels than in the control or those treated with GNPs gels.[25] When I-PRF was combined with DBBM, new bone formation occurred in the Schneiderian membrane area and the basal bone wall.[26] After 4 weeks, the GNPs-I-PRF group had higher scores in terms of trabecular bone and the volume of new bone formation but less trabecular separation than the control and GNP groups. Mu et al[25] concluded that GNPs-I-PRF hydrogels notably reduced

bone resorption in the treated sinus cavities. They also reported that, despite an initial increase in vascular formation and bone remodeling when DBBM was combined with I-PRF, there was no substantial difference in bone volume over time.[26] Yuan et al[27] recently investigated the effects of DBBM, GNPs, and I-PRF on angiogenesis, osteogenesis, and bone mass reduction in male dogs. Combining GNPs with I-PRF led to an increase in angiogenesis and woven bone formation, simultaneously reducing osteoclast activity in extraction sockets 2 weeks after surgery. At 8 weeks after the procedure, corticalization of the alveolar ridge crest had increased significantly.[27] Valladão et al[28] studied the impact of combining I-PRF/L-PRF, bone grafts, and membranes for bone augmentation in patients with horizontal or vertical bone defects necessitating dental implants. Radiographic evaluations utilizing cone-beam CT after an average period of 7.5±1.0 months demonstrated a notable enhancement in bone thickness ($p=0.001$) and height ($p=0.005$) when bone grafts were combined with PRF.[28] In 2020, Rao et al[29] investigated the impact of A-PRF and I-PRF in conjunction with an iliac bone graft in patients with a complete unilateral cleft alveolus. The Bergland criteria and periodontal parameters, including periodontal pocket depth and mobility indices, were assessed at 3 and 6 months. Patients who received a combination of iliac bone graft, A-PRF, and I-PRF demonstrated superior outcomes compared to those treated with an iliac bone graft alone.[29] We hypothesized that the combined use of biomaterials with I-PRF would allow the successful repair of bone defects in osteoporotic rats.

A critical early stage in bone mending is chemotaxis.[30,31] Platelet-derived growth factor, TGF-β, and other factors in I-PRF induce the chemotaxis of pre-osteoblasts to territories requiring bone revamping, in turn inducing osteogenic proliferation and differentiation. Angiogenesis is the key to furthering bone regeneration, as it allows for the differentiation of osteoblasts and osteoclasts during the formation of new bone.[32] Our results showed that ABG+I-PRF strongly stimulated osteoblast activity, accompanied by a substantial increase in the number of blood vessels. The micro-CT results supported the histology findings.

During the 4th week of healing, more positive signs of osteogenesis, increased vascularization, and a higher new bone volume ratio were observed in the ABG+I-PRF group than in the other groups. This faster rate of bone remodeling can be expected to lead to the formation of relatively mature bone within a short time. The combined effects of I-PRF, neovascularization, and

a surge in osteoblasts and osteoclasts support active bone remodeling and the early maturation of bone.[33,34] The results from the I-PRF+ABG group imply a role for I-PRF in mature bone formation as early as 4 weeks after treatment.

Bone healing tends to proceed at a slower pace in osteoporotic patients compared to individuals with healthy bone density. The current study demonstrated that I-PRF promoted bone regeneration in osteoporotic rats. Increased bone formation was observed in the PRF and autogenous bone groups among osteoporotic animals. This could be attributed to the release of growth factors from PRF.

In the recently literature review Miron et al[35] introduced the concept of C-PRF in their study. They demonstrated that using high g-force protocols (L-PRF) results in a concentration with a significant accumulation of leukocytes, platelets, and monocytes. Compared to the traditional I-PRF concentration, they showed an increase of over 500% in leukocytes and over 1500% in platelet counts.

Study limitations. Further studies are necessary to thoroughly understand the effects of PRF and its variants on osteoporotic animals. Further investigation is needed to explore the extended effects of I-PRF or C-PRF on bone regeneration in osteoporosis over time. Comparisons with other regenerative therapies and studies involving larger sample sizes will contribute to a more comprehensive understanding of the therapeutic benefits associated with I-PRF or C-PRF.

In conclusion, both micro-CT evaluations and the histopathologic analyses showed that the application of I-PRF+ABG is more successful in promoting new bone formation, as determined histologically, at the end of a 28-day healing period. A combined treatment consisting of I-PRF and ABG results in a higher regeneration capacity of osteoporotic bones, thus providing an effective strategy for bone formation in defect repair. However, further studies are required to understand more fully the process of new bone formation and augmentation in osteoporotic bone.

References

1. Ji Y, Wang L, Watts DC, Qiu H, You T, Deng F, et al. Controlled-release naringin nanoscaffold for osteoporotic bone healing. *Dent Mater* 2014; 30: 1263-1273.

2. Cosman F, de Beur SJ, LeBoff MS, Lewiecki EM, Tanner B, Randall S, et al. Clinician's guide to prevention and treatment of osteoporosis. *Osteoporos Int* 2014; 25: 2359-2381.

3. Ramalingam S, Al-Rasheed A, ArRejaie A, Nooh N, Al-Kindi M, Al-Hezaimi K. Guided bone regeneration in standardized calvarial defects using beta-tricalcium phosphate and collagen membrane: a real-time in vivo micro-computed tomographic experiment in rats. *Odontology* 2016; 104: 199-210.

4. Dohan Ehrenfest DM, Rasmusson L, Albrektsson T. Classification of platelet concentrates: from pure platelet-rich plasma (P-PRP) to leucocyte- and platelet-rich fibrin (L-PRF). *Trends Biotechnol* 2009; 27: 158-167.

5. Dohan Ehrenfest DM, Del Corso M, Diss A, Mouhyi J, Charrier JB. Three-dimensional architecture and cell composition of a Choukroun's platelet-rich fibrin clot and membrane. *J Periodontol* 2010; 81: 546-555.

6. Ghanaati S, Booms P, Orlowska A, Kubesch A, Lorenz J, Rutkowski J, et al. Advanced platelet-rich fibrin: a new concept for cell-based tissue engineering by means of inflammatory cells. *J Oral Implantol* 2014; 40: 679-689.

7. Miron RJ, Fujioka-Kobayashi M, Hernandez M, Kandalam U, Zhang Y, Ghanaati S, et al. Injectable platelet rich fibrin (i-PRF): opportunities in regenerative dentistry? *Clin Oral Investig* 2017; 21: 2619-2627.

8. Wang X, Zhang Y, Choukroun J, Ghanaati S, Miron RJ. Effects of an injectable platelet-rich fibrin on osteoblast behavior and bone tissue formation in comparison to platelet-rich plasma. *Platelets* 2018; 29: 48-55.

9. Choukroun J, Ghanaati S. Reduction of relative centrifugation force within injectable platelet-rich-fibrin (PRF) concentrates advances patients' own inflammatory cells, platelets and growth factors: the first introduction to the low speed centrifugation concept. *Eur J Trauma Emerg Surg* 2018; 44: 87-95.

10. Xu L, Ding Y, Lei C, Jiang W. The use of advance platelet-rich fibrin during immediate implantation for the esthetic replacement of maxillary anterior segment with chronic apical lesion. *IJSR* 2014; 3: 1368-1372.

11. Pathak H, Mohanty S, Urs AB, Dabas J. Treatment of oral mucosal lesions by scalpel excision and platelet-rich fibrin membrane grafting: a review of 26 sites. *J Oral Maxillofac Surg* 2015; 73: 1865-1874.

12. Anilkumar K, Geetha A, Umasudhakar, Ramakrishnan T, Vijayalakshmi R, Pameela E. Platelet-rich-fibrin: a novel root coverage approach. *J Indian Soc Periodontol* 2009; 13: 50-54.

13. Hoaglin DR, Lines GK. Prevention of localized osteitis in mandibular third-molar sites using platelet-rich fibrin. *Int J Dent* 2013; 2013: 875380.

14. Choukroun J, Diss A, Simonpieri A, Girard MO, Schoeffler C, Dohan SL, et al. Platelet-rich fibrin (PRF): a second-generation platelet concentrate. Part V: histologic evaluations of PRF effects on bone allograft maturation in sinus lift. *Oral Surg Oral Med Oral Pathol Oral Radiol Endod* 2006; 101: 299-303.

15. Lei Z, Xiaoying Z, Xingguo L. Ovariectomy-associated changes in bone mineral density and bone marrow haematopoiesis in rats. *Int J Exp Pathol* 2009; 90: 512-519.

16. Ferreira Sávio DS, Silva LMPD, Reis GGD, Denardi RJ, Costa NMMD, Chaves Furlaneto FA, et al. Effects of platelet-rich fibrin produced by 3 centrifugation protocols on bone neoformation in defects created in rat calvaria. *Platelets* 2023; 34: 2228417.

17. Durmuşlar MC, Türer A, Ballı U, Yılmaz Z, Önger ME, Çelik HH, et al. The effect of infliximab on bone healing in osteoporotic rats. *Eur J Inflamm* 2016; 14: 54-60.

18. Santić V, Cvek SZ, Sestan B, Bobinac D, Tudor A, Miletić D, et al. Treatment of tibial bone defect with rotational vascular periosteal graft in rabbits. *Coll Antropol* 2009; 33: 43-50.

19. Oberg S, Johansson C, Rosenquist JB. Bone formation after implantation of autolysed antigen extracted allogeneic bone in ovariectomized rabbits. *Int J Oral Maxillofac Surg* 2003; 32: 628-632.

20. Do Prado Ribeiro DC, de Abreu Figueira L, Issa JP, Dias Vecina CA, Josédias F, Da Cunha MR. Study of the osteoconductive capacity of hydroxyapatite implanted into the femur of ovariectomized rats. *Microsc Res Tech* 2012; 75: 133-137.

21. Durão SF, Gomes PS, Colaço BJ, Silva JC, Fonseca HM, Duarte JR, et al. The biomaterial-mediated healing of critical size bone defects in the ovariectomized rat. *Osteoporos Int* 2014; 25: 1535-1545.

22. Fujioka-Kobayashi M, Miron RJ, Hernandez M, Kandalam U, Zhang Y, Choukroun J. Optimized platelet-rich fibrin with the low-speed concept: growth factor release, biocompatibility, and cellular response. *J Periodontol* 2017; 88: 112-121.

23. Jasmine S, A T, Janarthanan K, Krishnamoorthy R, Alshatwi AA. Antimicrobial and antibiofilm potential of injectable platelet rich fibrin - a second-generation platelet concentrate - against biofilm producing oral staphylococcus isolates. *Saudi J Biol Sci* 2020; 27: 41-46.

24. Zhang J, Yin C, Zhao Q, Zhao Z, Wang J, Miron RJ, et al. Anti-inflammation effects of injectable platelet-rich fibrin via macrophages and dendritic cells. *J Biomed Mater Res A* 2020; 108: 61-68.

25. Mu Z, He Q, Xin L, Li Y, Yuan S, Zou H, et al. Effects of injectable platelet rich fibrin on bone remodeling in combination with DBBM in maxillary sinus elevation: a randomized preclinical study. *Am J Transl Res* 2020; 12: 7312-7325.

26. Mu Z, Chen K, Yuan S, Li Y, Huang Y, Wang C, et al. Gelatin nanoparticle-injectable platelet-rich fibrin double network hydrogels with local adaptability and bioactivity for enhanced osteogenesis. *Adv Healthc Mater* 2020; 9: e1901469.

27. Yuan S, Li Q, Chen K, Mu Z, Chen T, Wang H, et al. Ridge preservation applying a novel hydrogel for early angiogenesis and osteogenesis evaluation: an experimental study in canine. *J Biol Eng* 2021; 15: 19.

28. Amaral Valladão CA Jr, Freitas Monteiro M, Joly JC. Guided bone regeneration in staged vertical and horizontal bone augmentation using platelet-rich fibrin associated with bone grafts: a retrospective clinical study. *Int J Implant Dent* 2020; 6: 72.

29. Dayashankara Rao JK, Bhatnagar A, Pandey R, Arya V, Arora G, Kumar J, et al. A comparative evaluation of iliac crest bone graft with and without injectable and advanced platelet rich fibrin in secondary alveolar bone grafting for cleft alveolus in unilateral cleft lip and palate patients: a randomized prospective study. *J Stomatol Oral Maxillofac Surg* 2021; 122: 241-247.

30. Hosogane N, Huang Z, Rawlins BA, Liu X, Boachie-Adjei O, Boskey AL, et al. Stromal derived factor-1 regulates bone morphogenetic protein 2-induced osteogenic differentiation of primary mesenchymal stem cells. *Int J Biochem Cell Biol* 2010; 42: 1132-1141.

31. Wu B, Wang L, Yang X, Mao M, Ye C, Liu P, et al. Norepinephrine inhibits mesenchymal stem cell chemotaxis migration by increasing stromal cell-derived factor-1 secretion by vascular endothelial cells via NE/abrd3/JNK pathway. *Exp Cell Res* 2016; 349: 214-220.

32. Sivaraj KK, Adams RH. Blood vessel formation and function in bone. *Development* 2016; 143: 2706-2715.

33. Dohle E, El Bagdadi K, Sader R, Choukroun J, James Kirkpatrick C, Ghanaati S. Platelet-rich fibrin-based matrices to improve angiogenesis in an in vitro co-culture model for bone tissue engineering. *J Tissue Eng Regen Med* 2018; 12: 598-610.

34. Pichotano EC, de Molon RS, de Souza RV, Austin RS, Marcantonio E, Zandim-Barcelos DL. Evaluation of L-PRF combined with deproteinized bovine bone mineral for early implant placement after maxillary sinus augmentation: a randomized clinical trial. *Clin Implant Dent Relat Res* 2019; 21: 253-262.

35. Miron RJ, Chai J, Zhang P, Li Y, Wang Y, Mourão CFAB, et al. A novel method for harvesting concentrated platelet-rich fibrin (C-PRF) with a 10-fold increase in platelet and leukocyte yields. *Clin Oral Investig* 2020; 24: 2819-2828.